Organometallics **1997,** *16,* 5113−5115

Notes

H$^+$, $\mathrm{AuPPh_3}^+$, and $\mathrm{Hg\{Mo(CO)_3Cp\}}^+$ Show Different Sites of Attachment to $[\mathrm{Fe_4C(CO)_{12}}]^{2-}$ †

Roser Reina,‡ Olga Riba,‡ Oriol Rossell,*,‡ Miquel Seco,‡ Pilar Gómez-Sal,§ and
Avelino Martín§

*Departament de Química Inorgànica, Universitat de Barcelona, Martí i Franquès 1,
E-08028 Barcelona, Spain, and Departamento de Química Inorgánica, Universidad de Alcalá,
E-28071 Alcalá de Henares, Spain*

Received June 5, 1997⊗

*Summary: The reaction of the PPN$^+$ salt of $[Fe_4C(CO)_{12}]^{2-}$ with ClHgM (M = metal fragment) in CH_2Cl_2 gives the new hexanuclear carbide clusters (PPN)$[Fe_4C(CO)_{12}\{\mu\text{-}HgM\}]$ (M = $Mo(CO)_3Cp$ (**1**), $W(CO)_3Cp$ (**2**), $Mn(CO)_5$ (**3**), $Fe(CO)_2Cp$ (**4**), $Co(CO)_4$ (**5**)) in good yields. The X-ray crystal structure of **1** is without precedent in that a mercury atom bridges one of the two edges defined by wingtip and hinge iron atoms of the Fe_4C butterfly, giving a new skeletal isomer of an MFe_4C arrangement.*

Condensation reactions between anionic carbonyl clusters and cationic ligand−metal fragments have been shown to be an important route for the formation of metal clusters. The nature of the resulting compounds is not easily predicted if high-nuclearity cluster anions are used, because a range of interactions between them are possible. The butterfly cluster $[\mathrm{Fe_4C(CO)_{12}}]^{2-}$ is a good example of this. Thus, the bonding of this anion with cationic species, such as $\mathrm{AuPR_3}^+$ or H$^+$, occurs by overbridging the butterfly (position Z_1) or by bridging the hinge (position Z_2)[1,2] (Figure 1).

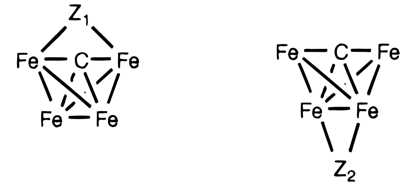

Figure 1.

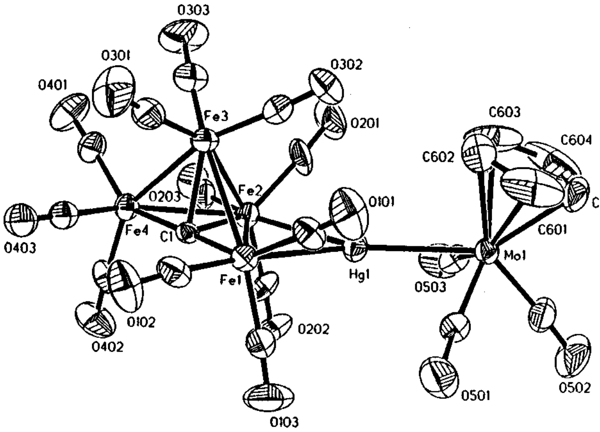

Figure 2. View of the molecular structure of the anionic cluster of **1** with the atomic numbering scheme.

Table 1. Selected Bond Distances (Å) and Angles (deg) for 1

Hg(1)−Fe(2)	2.694(2)	Hg(1)−Fe(1)	2.723(2)
Hg(1)−Mo(1)	2.759(10)	Fe(1)−C(1)	1.812(10)
Fe(1)−Fe(3)	2.648(2)	Fe(1)−Fe(2)	2.831(2)
Fe(2)−C(1)	1.921(9)	Fe(2)−Fe(3)	2.546(2)
Fe(2)−Fe(4)	2.625(2)	Fe(3)−C(1)	1.961(9)
Fe(3)−Fe(4)	2.631(2)	Fe(4)−C(1)	1.786(10)
Fe(2)−Hg(1)−Fe(1)	63.02(5)	Fe(2)−Hg(1)−Mo(1)	153.11(4)
Fe(1)−Hg(1)−Mo(1)	142.77(4)	C(1)−Fe(1)−Fe(3)	47.8(3)
C(1)−Fe(1)−Fe(2)	42.1(3)	Hg(1)−Fe(1)−Fe(2)	57.98(4)
C(1)−Fe(2)−Fe(3)	49.7(3)	C(1)−Fe(2)−Fe(4)	42.9(3)
Fe(4)−Fe(2)−Fe(1)	82.10(6)	Hg(1)−Fe(2)−Fe(1)	58.99(5)
C(1)−Fe(4)−Fe(2)	47.0(3)	Fe(4)−C(1)−Fe(2)	90.1(4)
Fe(1)−C(1)−Fe(2)	98.6(4)	Fe(4)−C(1)−Fe(3)	89.1(4)
Fe(1)−C(1)−Fe(3)	89.1(4)	Fe(2)−C(1)−Fe(3)	81.9(3)

Clusters showing both positions simultaneously occupied have also been reported.[3] While H$^+$ occupies position Z_2 without exception, the isolobal $\mathrm{AuPR_3}^+$ fragment[4] prefers Z_1. Thus, the isolobal analogy between $\mathrm{AuPR_3}^+$ and HgM$^+$ (where M is a metal fragment, such as $\mathrm{Mo(CO)_3Cp}$)[5] prompted us to identify the site preference of the bimetallic mercury unit toward the $\mathrm{Fe_4C}$ anion. We report here the unexpected site of attachment of the $\mathrm{Hg\{Mo(CO)_3Cp\}}^+$ unit to the $[\mathrm{Fe_4C(CO)_{12}}]^{2-}$ anion. Treatment of $(\mathrm{PPN})_2[\mathrm{Fe_4C(CO)_{12}}]$ with ClHgM in $\mathrm{CH_2Cl_2}$ afforded (PPN)$[\mathrm{Fe_4C(CO)_{12}}\{\mu\text{-HgM}\}]$ (M = $\mathrm{Mo(CO)_3Cp}$ (**1**), $\mathrm{W(CO)_3Cp}$ (**2**), $\mathrm{Mn(CO)_5}$ (**3**), $\mathrm{Fe(CO)_2Cp}$ (**4**), $\mathrm{Co(CO)_4}$ (**5**)) in good yields as shown in eq 1. **1** and **2** were isolated as brown microcrystalline

$$(\mathrm{PPN})_2[\mathrm{Fe_4C(CO)_{12}}] + \mathrm{ClHgM} \rightarrow (\mathrm{PPN})[\mathrm{Fe_4C(CO)_{12}}\{\mu\text{-HgM}\}] + (\mathrm{PPN})\mathrm{Cl} \tag{1}$$

solids and **3**−**5** as oils. The complexes were character-

---

† Dedicated to Prof. Pascual Royo on the occasion of his 60th birthday.

‡ Universitat de Barcelona.

§ Universidad de Alcalá.

⊗ Abstract published in *Advance ACS Abstracts,* October 1, 1997.

(1) Holt, E. M.; Whitmire, K. H.; Shriver, D. F. *J. Organomet. Chem.* **1981**, *213*, 125.

(2) Bogdan, P. L.; Horwitz, C. P.; Shriver, D. F. *J. Chem. Soc., Chem. Commun.* **1986**, 553.

(3) Johnson, B. F. G.; Kaner, D. A.; Lewis, J.; Raithby, P. R.; Rosales, M. J. *J. Organomet. Chem.* **1982**, *231,* C59.

(4) Lauher, J. W.; Wald, K. *J. Am. Chem. Soc.* **1981**, *103*, 7648.

(5) Reina, R.; Rossell, O.; Seco, M.; de Montauzon, D.; Zquiak, R. *Organometallics* **1994**, *13*, 4300. Rossell, O.; Seco, M.; Segalés, G.; Alvarez, S.; Pellinghelli, M. A.; Tiripicchio, A. *Organometallics* **1994**, *13*, 2205. Rossell, O.; Seco, M.; Reina, R.; Font-Bardía, M.; Solans, X. *Organometallics* **1994**, *13*, 2127. Rossell, O.; Seco, M.; Segalés, G.; Pellinghelli, M. A.; Tiripicchio, A.; de Montauzon, D. *Organometallics* **1997**, *16*, 236.

S0276-7333(97)00465-2 CCC: $14.00

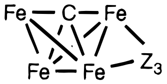

Figure 3.

ized spectroscopically, and a single-crystal X-ray structure analysis of **1** was carried out. The structure of the cluster anion is shown in Figure 2. Selected bond distances and angles are listed in Table 1.

The four iron atoms are in a butterfly arrangement, while surprisingly, the Hg atom bridges one of the two edges defined by wingtip and hinge iron atoms (position Z_3, Figure 3).

This unexpected structural feature leads to a new metal cluster framework, which can be considered as the third skeletal isomer of the clusters generated from a carbide-butterfly M_4C skeleton. The molecule is chiral (C_1) because the incorporation of the HgM fragment breaks the C_{2v} symmetry of the dianion. The $HgMo(CO)_3Cp$ portion of the molecule has the typical irregular “four-legged piano-stool” structure. The carbide atom occupies the cavity of the Fe_4 metal core and is bonded to all four metal atoms almost collinearly to the wingtip atoms. Interestingly, although the 11 CO groups are terminal, the CO(203) ligand appears asymmetrically bridging the Fe(2)−Fe(4) edge.

Although mercury compounds are known to participate in a wide range of ligand-redistribution reactions,[6] clusters **1**−**5** are inert to such processes, probably because of the presence of the negative charge, as has been reported for other mercury systems.[7]

The electrochemical properties of **1** and **2** have been studied in the electroactivity range of the solvent (CH_2Cl_2).[8] The cyclic voltammetric measurements show two electrode processes: (i) a well-defined wave corresponding to a quasi-reversible oxidation process of one electron, with $E_{1/2}(\mathbf{1}) = 0.36$ V and $E_{1/2}(\mathbf{2}) = 0.34$ V versus SCE, and (ii) an irreversible reduction process of two electrons with $E_{p,c}(\mathbf{1}) = -1.31$ V and $E_{p,c}(\mathbf{2}) = -1.32$ V versus SCE. A typical tube EPR oxidation experiment at −78 °C with $[FeCp_2][PF_6]$ allowed us to detect the radical species $[Fe_4C(CO)_{12}(\mu\text{-HgM})]^{\bullet}$. The X-band EPR spectrum (identical for both complexes) consists of a single strong resonance centered at *ca.* 3267 G ($g = 2.06$) flanked by two satellite signals assigned to a hyperfine coupling with ^{199}Hg ($a = 108$ G). The hyperfine coupling indicates that the unpaired electron density in the neutral radical is primarily located in the Fe_4Hg core, in agreement with the theoretical studies, where the HOMO orbital is mainly formed by the atomic orbitals of these metals.

In conclusion, we have shown that the butterfly edge defined by a wingtip and a hinge iron atom is also prone to be bridged by a ligand−metal fragment. This means that the third skeletal isomer for the clusters derived from $[Fe_4C(CO)_{12}]^{2-}$ has been isolated for the first time.

Experimental Part

Preparation of Complexes. The following standard procedure was used to synthesize **1**. $ClHgMo(CO)_3Cp$ (0.14 g, 0.28 mmol) and $TlBF_4$ (0.08 g, 0.28 mmol) were added to a suspension of $[PPN]_2[Fe_4C(CO)_{12}]$ (0.47 g, 0.28 mmol) in CH_2Cl_2 (15 mL) at −5 °C. The brown solution was stirred for 45 min, and 60 mL of cold ether was added to precipitate TlCl and $(PPN)BF_4$. The mixture was filtered, and ether was removed under vacuum. A 20 mL portion of isopropyl alcohol was added to the remaining solution, and the volume was reduced to approximately 20 mL by slow evaporation under low pressure. The solution was left to stand at −30 °C overnight, and a brown microcrystalline solid was obtained. Yields for **1** and **2** were 75 and 70%, respectively. **3**−**5**: With the procedure described above, $[PPN]_2[Fe_4C(CO)_{12}]$ was allowed to react with $ClHgMn(CO)_5$, $ClHgFe(CO)_2Cp$, and $ClHgCo(CO)_4$, respectively, and hexane was then added to produce brown oils in yields of 40, 45, and 37%, respectively. **1**: Anal. Calcd for $C_{57}H_{35}Fe_4HgMoNO_{15}P_2$: C, 43.99; H, 2.25; N, 0.90. Found: C, 44.10; H, 2.29; N, 0.98. MS (negative ES, 80 eV; *m/z* (%)): 1018.2 (100) $[M^-]$. ^1H NMR (δ, CD_2Cl_2): 5.41 (s, 5H; Cp), 7.48−7.67 (m, 30H; Ph). ^{13}C NMR (δ, CD_2Cl_2): 88.9 (Cp), 126.5−134.1 (Ph), 214.3 (CO), 217.7 (CO), 475.5 (C); IR (CH_2Cl_2, cm^{-1}): ν(CO) 2055 (w), 2005 (s), 1988 (vs), 1975 (sh), 1943 (m), 1900 (w), 1879 (w). **2**: Anal. Calcd for $C_{57}H_{35}Fe_4HgNO_{15}P_2W$: C, 41.64; H, 2.13; N, 0.85. Found: C, 41.71; H, 2.19; N, 0.87. MS (negative ES, 80 eV; *m/z* (%)): 1104.5 (100) $[M^-]$. ^1H NMR (δ, CD_2Cl_2): 5.51 (s, 5H; Cp), 7.48−7.66 (m, 30H; Ph). ^{13}C NMR (δ, CD_2Cl_2): 87.6 (Cp), 126.6−134.1 (Ph), 214.5 (CO), 217.9 (CO), 472.8 (C). IR (CH_2Cl_2, cm^{-1}): ν(CO) 2054 (w), 2004 (s), 1988 (vs), 1974 (sh), 1945 (m), 1890 (w), 1872 (w). **3**: MS (negative ES, 80 eV; *m/z* (%)): 967.8 (100) $[M^-]$. ^{13}C NMR (δ, CD_2Cl_2): 126.5−134.1 (Ph), 214.1 (CO), 217.5 (CO), 217.7 (CO), 477.1 (C). IR (CH_2Cl_2, cm^{-1}): ν(CO) 2091 (w), 2081 (w), 2049 (m), 2009 (vs), 1994 (vs), 1976 (s), 1944 (sh) cm^{-1}. **4**: MS (negative ES, 80 eV; *m/z* (%)): 951.2 (100) $[M^-]$. ^1H NMR (δ, CD_2Cl_2): 4.88 (s, 5H; Cp), 7.48−7.65 (m, 30H; Ph). ^{13}C NMR (δ, CD_2Cl_2): 80.7 (Cp), 126.6−134.1 (Ph), 213.9 (CO), 215.2 (CO), 218.5 (CO), 472.3 (C). IR (in CH_2Cl_2, cm^{-1}): ν(CO) 2052 (w), 2002 (vs), 1987 (s), 1972 (s), 1944 (m) cm^{-1}. **5**: MS (negative ES, 80 eV; *m/z* (%)): 944.0 (100) $[M^-]$. 13C NMR (δ, CD_2Cl_2): 126.4−134.0 (Ph), 207.2 (CO), 212.9 (CO), 216.3 (CO), 482.1 (C). IR (CH_2Cl_2, cm^{-1}): ν(CO) 2073 (w), 2052 (m), 2012 (vs), 1996 (vs), 1976 (s) cm^{-1}.

Table 2. Crystallographic Data for 1

mol formula	$C_{57}H_{35}Fe_4HgMoNO_{15}P_2$
fw	1555.73
cryst syst	monoclinic
space group	$P2_1/c$
a (Å)	20.146(5)
b (Å)	19.377(3)
c (Å)	15.760(3)
β (deg)	111.66(1)
V (Å^3)	5718(2)
Z	4
T (K)	292
D_{calcd} (g cm^{-3})	1.807
F(000)	3040
GOF(F^2)	1.010
R1[a]	0.059
wR2[b]	0.143
index range	h, 0−23; k, −22 to 0; l, −18 to +18

[a] $R1 = \sum||F_o| - |F_c||/[\sum|F_o|]$. [b] $wR2 = \{[\sum w(F_o^2 - F_c^2)^2]/[\sum w(F_o^2)^2]\}^{1/2}$.

X-ray Structure Determination of 1. The data were collected on an Enraf-Nonius CAD4 automatic four-circle diffractometer with bisecting geometry, equipped with a graphite-oriented monochromator and Mo Kα radiation ($\lambda = 0.710\,73$ Å). Crystallographic data are summarized in Table 2. Intensity measurements were performed by $\omega-\theta$ scans in the range $2° < 2\theta < 50°$ at 19 °C on a dark brown crystal of dimensions 0.40 × 0.25 × 0.20 mm. Intensities were corrected for Lorentz and polarization effects in the usual manner. Absorption was corrected by the ψ-scan technique (maximum and minimum transmission factors 1.000 and 0.409). No extinction correction was made. Of the 10 358 measured

---

(6) Rosenberg, E.; Wang, J. *Organometallics* **1988**, *7*, 1093 and references therein.

(7) Gade, L. H. *Angew. Chem., Int. Ed. Engl.* **1993**, *32*, 24.

(8) Electrochemical data are referred to CH_2Cl_2 solutions (5×10^{-4} M) of **1** and **2** containing 0.1 M $[n\text{-}Bu_4N][PF_6]$ at a scan rate of 0.1 V/s.

reflections, 10 056 were independent. Largest minimum and maximum in the final difference Fourier synthesis: −0.768 and 1.148 e Å^{-3}, R1 = 0.059 and wR2 = 0.143 (for 5814 reflections with $F > 4\sigma(F)$). The values of R1 and wR2 are defined as R1 = $\sum||F_o| - |F_c||/[\sum|F_o|]$ and wR2 = $\{[\sum w(F_o^2 - F_c^2)^2]/[\sum w(F_o^2)^2]\}^{1/2}$. The structure was solved by direct methods (SHELXS-90)[9] and refined by least squares against F^2 (SHELXL-93).[10] All non-hydrogen atoms were refined anisotropically, and the hydrogen atoms were positioned geometrically and refined by using a riding model. Calculations were carried out on an ALPHA AXP (Digital) workstation.

Acknowledgment. This work was supported by the DGICYT (Project PB93-0766) and Universidad de Alcalá (Project 001/97). We thank Dominique de Montauzonfor his experimental assistance in the electrochemical studies.

Supporting Information Available: Tables of final values of atomic coordinates for the non-hydrogen atoms, calculated coordinates and isotropic thermal parameters for the hydrogen atoms, anisotropic thermal parameters for the non-hydrogen atoms, and a all bond distances and angles (8 pages). Ordering information is given on any current masthead page.

OM9704657

---

(9) Sheldrick, G. M. *Acta Crystallogr., Sect. A* **1990,** *46*, 467.

(10) Sheldrick, G. M. SHELXL 93; University of Göttingen, Göttingen, Germany, 1993.